

## **EFFECT OF MAGNETIC FIELD ON THE VOLTAGE OUTPUT OF TRIBOELECTRIC NANOGENERATOR**

**El-Shazly M. H.<sup>1</sup>, Al-Kabbany A. M.<sup>2</sup>, Ali W. Y.<sup>2</sup>, Ali A. S.<sup>3</sup> and Massoud M. A.<sup>4</sup>**

<sup>1</sup>Department of Mechanical Design and Production Engineering, Faculty of Engineering, Cairo University, Giza, Egypt.

<sup>2</sup>Department of Production Engineering and Mechanical Design, Faculty of Engineering, Minia University, Minia 61111, Egypt.

<sup>3</sup>Mechanical Engineering Dept., Faculty of Engineering, Suez Canal University, EGYPT.

<sup>4</sup>Biomedical Engineering Department, Minia University, P. N. 61111, El-Minia, EGYPT.

### **ABSTRACT**

The present work discusses the effect of magnetic field on the voltage output of a triboelectric nanogenerator (TENG) based on triboelectrification and magnetic field. One of the major factors influencing the performance of the TENG is the position of the permanent magnets relative to the triboelectrified area. In the present study, experiments were carried out to investigate the proper places of the permanent magnets relative to the tested area. The voltage difference between the surfaces of polytetrafluoroethylene (PTFE) and rabbit fur was measured after contact-separation and sliding.

When the magnets were placed on the top of the PTFE film, the strength of magnetic field is concentrated above the PTFE film, while the presence of the steel sheet under PTFE film reduced the magnetic field strength because steel shield attracts and redirects the field lines out of the sliding area. It was found that the increase of magnetic fields caused significant voltage increase. Besides, voltage displayed lower values by contact-separation than that measured for sliding. When the magnets were placed under the PTFE film, voltage decreased for contact and separation. The best results were observed for placing magnets above and under PTFE film, where higher voltage values were measured. Finally, replacing the steel sheet by PMMA generated significant voltage increase. Based on that observation, it is recommended to apply nonmagnetic materials in the design of hybrid electromagnetic triboelectric nanogenerator.

### **KEYWORDS**

**Magnetic field, voltage, triboelectric nanogenerator, induction.**

## **INTRODUCTION**

The triboelectric effect occurs when two surfaces come into contact with one another, where charges can be transferred from one surface to the other, [1 - 5]. The intensity and sign of the charges transferred is determined by the triboelectric series, that ranks materials according to their likelihood of obtaining a positive charge upon contact with another material, [6 - 8]. Despite its old history, the exact mechanism by which the process of triboelectrification is still unknown, with ion transfer being a likely explanation, [9].

The triboelectric effect can be a blessing or a curse. It can cause fires, [10, 11], or damage electronics, [12, 13]. In those cases, it can be reduced by multiple methods, such as blending two materials opposite to each other in the triboelectric series in one surface, [14 - 16]. However, it can be used to defend against viruses, [17 - 20], and it can be used to make multiple devices, such as the Van de Graff generator, [21], and the triboelectric nanogenerator (TENG), [22 - 24]. TENGs use a combination of triboelectrification and electrostatic induction to induce a voltage between two terminals, a terminal can be a dielectric connected to an electrode, just an electrode, or an electric ground. TENGs can be used in multiple ways, as energy harvesters, [25 - 28], or as self-powered sensors, [29 - 32].

Electromagnetic induction is one of the oldest ways of converting mechanical energy into electrical energy, other than its well-known applications, it has been used to make hybrid electromagnetic-TENGs, [33 - 39]. This would allow for the creation of devices with higher efficiency than either TENGs or electromagnetic generators.

The present work investigates the effect of magnetic lines distribution on the voltage output of a hybrid electromagnetic triboelectric nanogenerator (TENG) made from a PTFE and a rabbit fur because they are both opposite to each other in the triboelectric series. The proposed TENG can harvest mechanical energy by combining contact electrification and electrostatic induction.

## **EXPERIMENTAL**

The test specimens consisted of wooden cube of  $40 \times 40 \times 40 \text{ mm}^3$  coated by aluminium film (Al) of 0.25 mm thickness. Then rabbit fur was adhered to the Al film representing the first dielectric surface. The tested counterface was in form of PTFE film adhered to steel sheet of 0.3 mm thickness (second terminal) representing the second dielectric surface. The voltage difference was measured between the steel surface and Al film. Further experiments were carried out to investigate the effect of replacing the steel sheet by polymethyl methacrylate (PMMA) sheet of 0.3 mm thickness coated by Al film (second terminal) to avoid the shielding effect of the steel. The load was applied by the weight of the wooden block (0.5 N). The test procedure consisted of contact-separation and sliding. In contact-separation, the load is applied for 5 seconds followed by the measurement of the voltage. The sliding distance was 100 mm. The magnetic field was supplied by permanent magnets that produce their own persistent magnetic strength. They are made of ferromagnetic materials, such as iron and nickel, that have been magnetized, and they have both a north and a south

pole. The intensity of the magnetic field was 20, 60, 100 mG. The details of the test specimens and the test rig are shown in Fig. 1. The experiments were repeated five times to measure the voltage difference.

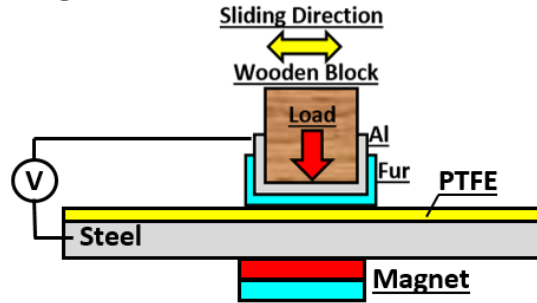


Fig. 1 Arrangement of test procedure.

## RESULTS AND DISCUSSION

When the magnets were placed on the top of the PTFE film, the magnetic field distribution is illustrated in Fig. 2. The intensity of the lines of magnetic field is concentrated above the PTFE film. Due to the presence of the steel sheet under PTFE film as ferromagnetic steel that has high magnetic permeability and can easily absorb and redirect magnetic fields, the effect of magnetic field under steel sheet decreased. It is known that steel shield attracts, channels the field lines and reduces the magnetic field strength. Steel is ferromagnetic and can be used to redirect shields.

Voltage generated from contact-separation and sliding when magnets are placed on the top of the PTFE film is shown in Fig. 3. It is seen that voltage difference generated from by contact-separation displayed lower values than that recorded for sliding. The highest voltage values recorded at 160 mG field strength for contact-separation and sliding were 1050 and 1280 mV respectively. In addition, the increase of magnetic fields caused significant voltage increase. This performance may be attributed to the double layer of ESC generated on the contact surfaces that induced an extra electric field on the sliding surfaces leading to the voltage increase. The movement of ESC generated from contact-separation and sliding generates a magnetic field that induces an electric current. Magnetic fields are often represented in field lines, where their density indicates the strength of the field. The higher dense the lines, the stronger the field.

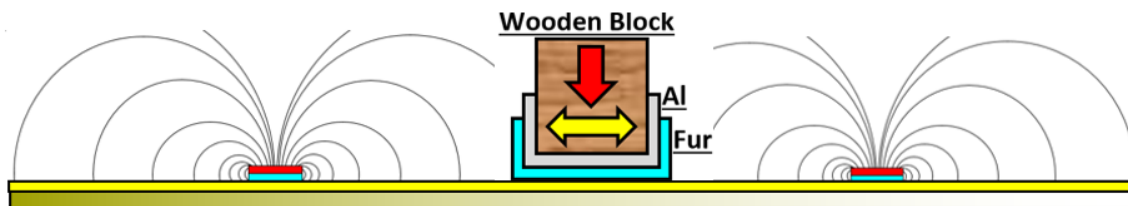


Fig. 2 Distribution of the magnetic field when the magnets are placed on the top of the PTFE film.

It is seen that, as the magnetic flux density increased, the output voltage of the device increased. It can also be noticed that when the magnets were placed under the PTFE film, Fig. 4, the output voltage drastically decreased in case of contact and separation compared to the condition of the magnets being above the PTFE film, Fig. 5. As for sliding, voltage recorded relatively higher values than that observed in Fig. 3. It seems that in the case of sliding, the number of magnetic field lines cut by the movement of rabbit fur increased. In spite of the decrease of the magnetic flux density by the effect of the shielding action of the steel sheet above the PTFE film, the voltage generated from sliding recorded higher values up to 1480 mV at 160 mG compared to that measured when the magnets were above the PTFE film. That may be attributed to the closer distance of the sliding object from the magnetic field lines.

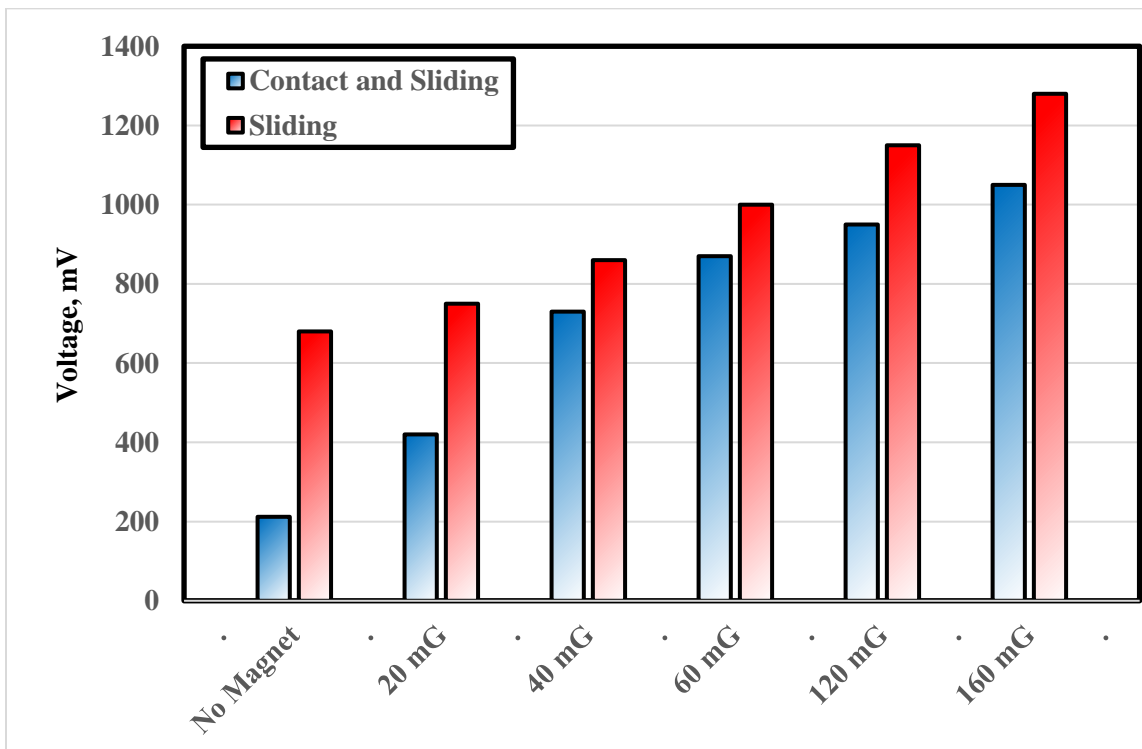


Fig. 3 Voltage generated from contact-separation and sliding when magnets are placed on the top of the PTFE film.

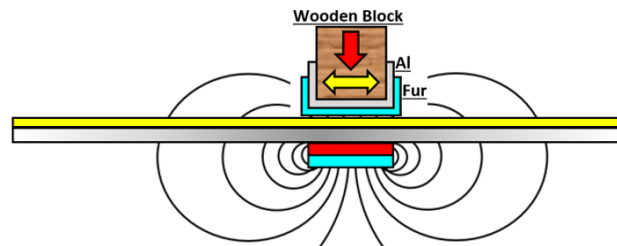


Fig. 4 Distribution of the magnetic field when the magnets are placed under the PTFE film.

When the magnets were placed above and under PTFE film, Fig. 6, higher values of voltage were measured, Fig. 7. This behavior can be explained on the bases that the magnets generated more uniform and complex field shape that would allow for the rabbit fur electrode to cut more field lines. However, the voltage generated via contact and separation was much lower than that observed for sliding. That performance can be attributed to the fact that the moving electric charge generated on the rabbit fur caused the generation of extra magnetic field. Then the magnetic field induced electric charge movement and produced an extra electric current.

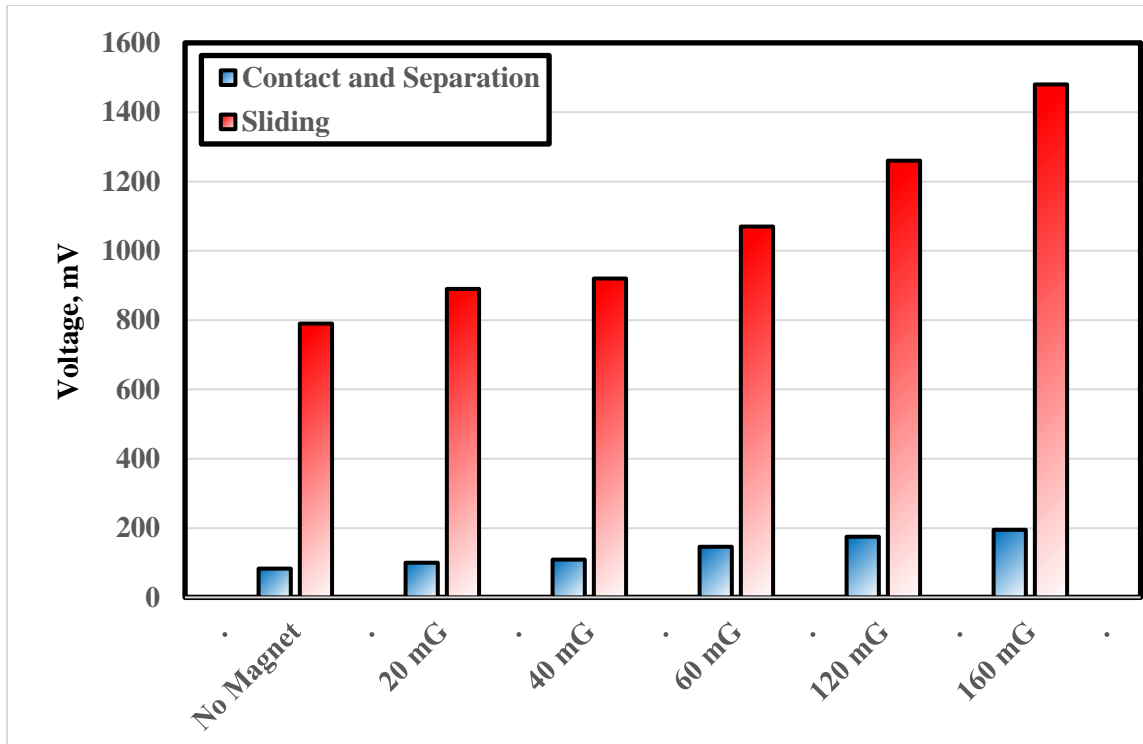


Fig. 5 Voltage generated from contact-separation and sliding when magnets are placed under the PTFE film.

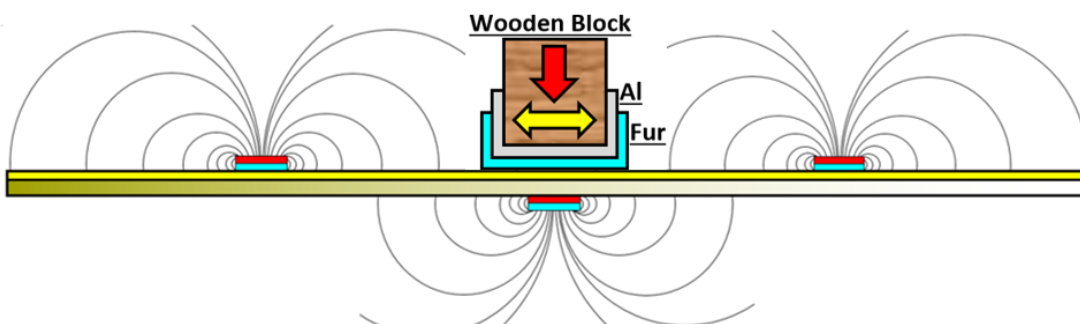
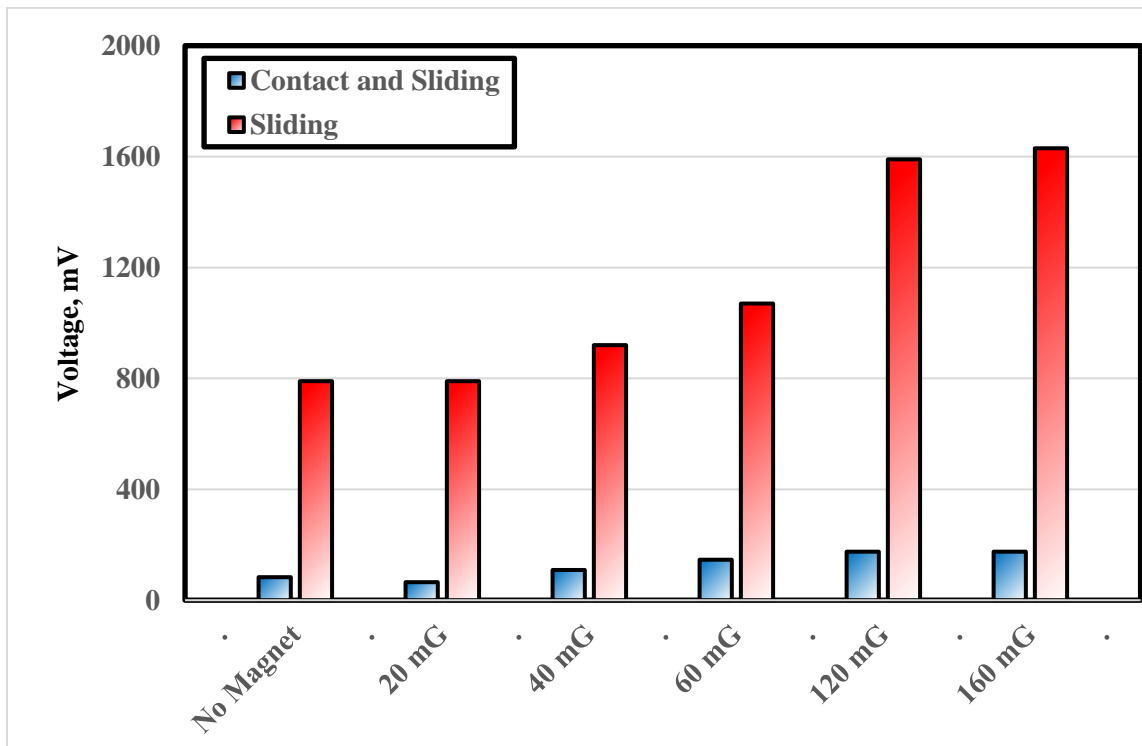
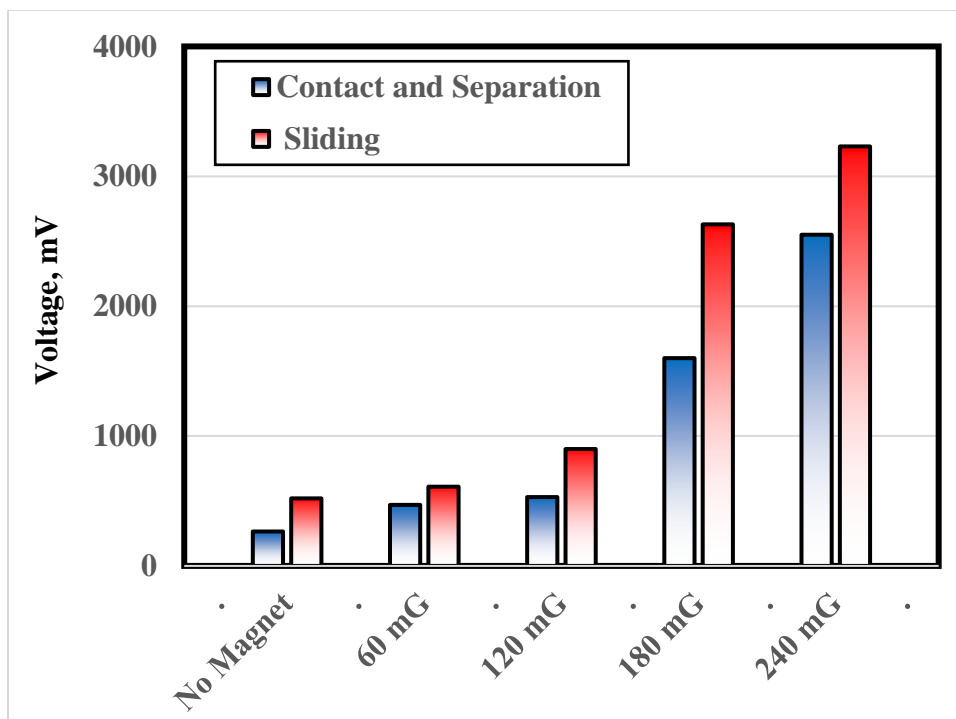


Fig. 6 Distribution of the magnetic field when the magnets are placed above and under the PTFE film.



**Fig. 7 Voltage generated from contact-separation and sliding when magnets are placed above and under the PTFE film.**



**Fig. 8 Voltage generated from contact-separation and sliding when magnets are placed under the PTFE film, where the steel sheet was replaced by PMMA sheet.**

The results of experiments carried out to investigate the effect of replacing the steel sheet by PMMA sheet on voltage generated from contact-separation and sliding when magnets are placed above and under the PTFE film are shown in Fig. 8. It is known that magnetic shielding does not block a magnetic field but it can redirect the lines of flux during traveling from north pole to south pole of the magnet. The presence of PMMA sheet allows the lines of magnetic field to flow from one pole of the magnet to the other with the same intensity, while steel sheet reduces the ambient field strength. The generated voltage represented relatively higher values than observed for that shielded by steel sheet. When the field strength was 240 mG, the values of generated voltage were 2550 and 3230 mV for contact-separation and sliding respectively. Based on that observation, it is recommended to use nonmagnetic materials as substrates in the design of hybrid electromagnetic triboelectric nanogenerator.

## CONCLUSIONS

1. The increase of magnetic fields caused significant voltage increase.
2. When magnets were placed on the top of the PTFE film, voltage difference displayed lower values by contact-separation than that recorded for sliding.
3. When the magnets were placed under the PTFE film, voltage drastically decreased for contact-separation compared to the condition of the magnets being above the PTFE film, while at sliding, voltage recorded relatively higher values.
4. Placing magnets above and under PTFE film, higher values of voltage were measured.
5. Replacing the steel sheet by PMMA generated remarkable voltage increase compared to that observed for steel sheet. Therefore, it is recommended to apply nonmagnetic materials in the parts of hybrid electromagnetic triboelectric nanogenerator.

## REFERENCES

1. Al-Qaham Y., Mohamed M. K., and Ali W. Y., "Electric static charge generated from the friction of textiles", *Journal of the Egyptian Society of Tribology*, Vol. 10, No. 2, pp. 45 - 56, (2013).
2. Naik S., Mukherjee R., and Chaudhuri B., "Triboelectrification: A review of experimental and mechanistic modeling approaches with a special focus on pharmaceutical powders", *International journal of pharmaceutics*, Vol. 510, No. 1, pp. 375 - 385, (2016).
3. Lowell J., and Rose-Innes A., "Contact electrification", *Advances in Physics*, Vol. 29, No. 6, pp. 947 - 1023, (1980).
4. Badran A. H., Fouly A., Ali W. Y., and Ameer A. K., "Electrostatic Charges Generated on the Medical Clothes", *Journal of the Egyptian Society of Tribology*, Vol. 18, No. 2, pp. 15 - 26, (2021).
5. Ali A. S., "Triboelectrification of Synthetic Strings", *Journal of the Egyptian Society of Tribology*, Vol. 16, No. 2, pp. 26 - 36, (2019).
6. Zou H., Zhang Y., Guo L., Wang P., He X., Dai G., Zheng H., Chen C., Wang A. C., Xu C., et al., "Quantifying the triboelectric series", *Nature communications*, Vol. 10, No. 1, p. 1427, (2019).

7. Diaz A., and Felix-Navarro R., “A semi-quantitative tribo-electric series for polymeric materials: the influence of chemical structure and properties”, *Journal of Electrostatics*, Vol. 62, No. 4, pp. 277 - 290, (2004).
8. Burgo T. A., Galembeck F., and Pollack G. H., “Where is water in the triboelectric series?”, *Journal of Electrostatics*, Vol. 80, pp. 30 - 33, (2016).
9. McCarty L. S., and Whitesides G. M., “Electrostatic charging due to separation of ions at interfaces: contact electrification of ionic electrets”, *Angew. Chem. Int. Ed.*, Vol. 47, No. 12, pp. 2188 - 2207, (2008).
10. Gabor D., Radu S. M., Ghicioi E., Paraian M., Jurca A. M., Vatavu N., Paun F., and Popa C. M., “Study of methods for assessment of the ignition risk of dust/air explosive atmospheres by electrostatic discharge”, *Calitatea*, Vol. 20, No. S1, p. 93, (2019).
11. Glor M., and Thurnherr P., “Ignition Hazards Caused by Electrostatic Charges in Industrial Processes”, *Thuba Ltd*, (2015).
12. Von Pidoll U., “An overview of standards concerning unwanted electrostatic discharges”, *Journal of Electrostatics*, Vol. 67, No. 2-3, pp. 445 - 452, (2009).
13. Tian H., and Lee J. J., “Electrostatic discharge damage of MR heads”, *IEEE transactions on magnetics*, Vol. 31, No. 6, pp. 2624 - 2626, (1995).
14. Al-Kabbany A. M., and Ali W. Y., “Reducing the Electrostatic Charge of Polyester by Blending by Polyamide Strings”, *Journal of the Egyptian Society of Tribology*, Vol. 16, No. 4, pp. 36 - 44, (2019).
15. Ali A. S., Al-Kabbany A. M., Ali W. Y., and Samy A. M., “Reducing the Electrostatic Charge Generated from Sliding of Rubber on Polyethylene Artificial Turf”, *Journal of the Egyptian Society of Tribology*, Vol. 17, No. 2, pp. 40 - 49, (2020).
16. Ali A. S., El-Sherbiny Y. M., Ali W. Y., and Ibrahim R. A., “Selection of Floor Materials in Hospitals to Resist Covid-19”, *Journal of the Egyptian Society of Tribology*, Vol. 18, No. 1, pp. 40 - 51, (2021).
17. Ali A. S., Al-Kabbany A. M., Ali W. Y., and Badran A. H., “Triboelectrified Materials of Facemask to Resist Covid-19”, *Journal of the Egyptian Society of Tribology*, Vol. 18, No. 1, pp. 52 - 62, (2021).
18. Ali A. S., Al-Kabbany A. M., Ali W. Y., and Ibrahim R. A., “Proper Material Selection of Medical Safety Goggles”, *Journal of the Egyptian Society of Tribology*, Vol. 18, No. 2, pp. 1 - 14, (2021).
19. Al-Kabbany A. M., Ali W. Y., and Ali A. S., “Proposed Materials for Face Masks”, *Journal of the Egyptian Society of Tribology*, Vol. 18, No. 3, pp. 35 - 41, (2021).
20. Al-Kabbany A. M., Ali W. Y., and Ali A. S., “Proper Selection Materials of Face Shields, Eyeglasses and Goggles”, *Journal of the Egyptian Society of Tribology*, Vol. 18, No. 3, pp. 42 - 51, (2021).
21. Furfari F. A. “A history of the Van de Graaff generator”, *IEEE Industry Applications Magazine*, Vol. 11, No. 1, pp. 10–14, (2005).
22. Fan F.-R., Tian Z.-Q., and Wang Z. L., “Flexible triboelectric generator”, *Nano Energy*, Vol. 1, No. 2, pp. 328 - 334, (2012).
23. Goh Q. L., Chee P., Lim E. H., and Liew G. G., “Self-powered pressure sensor based on microfluidic triboelectric principle for human–machine interface applications”, *Smart Materials and Structures*, Vol. 30, No. 7, p. 075012, (2021).



24. Zhang R., Hummelgard M., Ortegren J., Olsen M., Andersson H., Yang Y., Olin H., and Wang Z. L., "Utilising the triboelectricity of the human body for human-computer interactions", *Nano Energy*, Vol. 100, , p. 107503, (2022).
25. Yang Y., Zhu G., Zhang H., Chen J., Zhong X., Lin Z.-H., Su Y., Bai P., Wen X., and Wang Z. L., "Triboelectric nanogenerator for harvesting wind energy and as self-powered wind vector sensor system", *ACS nano*, Vol. 7, No. 10, pp. 9461 - 9468, (2013).
26. Han J., Feng Y., Chen P., Liang X., Pang H., Jiang T., and Wang Z. L., "Wind-driven soft-contact rotary triboelectric nanogenerator based on rabbit fur with high performance and durability for smart farming", *Advanced Functional Materials*, Vol. 32, No. 2, p. 2108580, (2022).
27. Zhang H., Yang Y., Su Y., Chen J., Adams K., Lee S., Hu C., and Wang Z. L., "Triboelectric nanogenerator for harvesting vibration energy in full space and as self-powered acceleration sensor", *Advanced Functional Materials*, Vol. 24, No. 10, pp. 1401 - 1407, (2014).
28. Cheng P., Guo H., Wen Z., Zhang C., Yin X., Li X., Liu D., Song W., Sun X., Wang J., et al., "Largely enhanced triboelectric nanogenerator for efficient harvesting of water wave energy by soft contacted structure", *Nano Energy*, Vol. 57, pp. 432 - 439, (2019).
29. Meng B., Tang W., Too Z.-h., Zhang X., Han M., Liu W., and Zhang H., "A transparent single-friction-surface triboelectric generator and selfpowered touch sensor", *Energy & Environmental Science*, Vol. 6, No. 11, pp. 3235 - 3240, (2013).
30. Lei H., Xiao J., Chen Y., Jiang J., Xu R., Wen Z., Dong B., and Sun X., "Bamboo-inspired self-powered triboelectric sensor for touch sensing and sitting posture monitoring", *Nano Energy*, Vol. 91, p. 106670, (2022).
31. Pu X., Tang Q., Chen W., Huang Z., Liu G., Zeng Q., Chen J., Guo H., Xin L., and Hu C., "Flexible triboelectric 3D touch pad with unit subdivision structure for effective XY positioning and pressure sensing", *Nano Energy*, Vol. 76, p. 105047, (2020).
32. Haque R. I., Chandran O., Lani S., and Briand D., "Self-powered triboelectric touch sensor made of 3D printed materials", *Nano Energy*, Vol. 52, pp. 54 - 62, (2018).
33. Chen Y., Cheng Y., Jie Y., Cao X., Wang N., and Wang Z. L., "Energy harvesting and wireless power transmission by a hybridized electromagnetic-triboelectric nanogenerator", *Energy & Environmental Science*, Vol. 12, No. 9, pp. 2678 - 2684, (2019).
34. Quan T., Wang Z. L., and Yang Y., "A shared-electrode-based hybridized electromagnetic-triboelectric nanogenerator", *ACS Applied Materials & Interfaces*, Vol. 8, No. 30, pp. 19 573 - 19 578, (2016).
35. Qin K., Chen C., Pu X., Tang Q., He W., Liu Y., Zeng Q., Liu G., Guo H., and Hu C., "Magnetic array assisted triboelectric nanogenerator sensor for real-time gesture interaction", *Nano-micro letters*, Vol. 13, pp. 1 - 9, (2021).
36. Ali A. S., Al-Kabbany A. M., and Ali W. Y., "Voltage Generated From Triboelectrification of Rabbit Fur and Polymeric Materials", *Journal of the Egyptian Society of Tribology*, Vol. 19, No. 3, pp. 10 - 18, (2022).
37. Zhang R., and Olin H., "Material choices for triboelectric nanogenerators: a critical review", *EcoMat*, Vol. 2, No. 4, p. e12062, (2020).

- 38. Ali A. S., Youssef M. M., Ali W. Y. and Elzayady N., “Triboelectric Nanogenerator Based on Contact and Separation as well as Sliding of Polyamide on Polytetrafluoroethelene”, Journal of the Egyptian Society of Tribology, Vol. 20, No. 1, January 2023, pp. 32 – 40, (2023).**
- 39. Ali A. S., Youssef M. M., Ali W. Y. and Rashed A., “Enhancing the Efficiency of Triboelectric Nanogenerator by Electrostatic Induction”, Journal of the Egyptian Society of Tribology, Vol. 20, No. 1, January 2023, pp. 41 – 50, (2023).**